

# Corrections to “A Single-Element Plane Grating Monochromator”

Michael C. Hettrick

Hettrick Scientific, Fuchu-shi Tokyo 183-0002 Japan

Corresponding author: [hettrickscientific@gmail.com](mailto:hettrickscientific@gmail.com)

**Abstract:** The author made three errors in a recent publication [M.C. Hettrick, “A Single-Element Plane Grating Monochromator”, *Photonics* 3(1), no. 3, 1-44 (2016)] and regrets any misunderstanding they may have caused. To maintain the rigor of the new light-path expansion method introduced therein, the author herein provides the necessary corrections and explanations.

© 2016 by the author.

In a recent publication [1], Equation (27) omitted a factor  $\eta$ , and should read as follows:

$$\begin{aligned} \partial B_{ij}/\partial(\Delta\sigma) &= \frac{\eta}{2} [\partial_B t_{ij}/\partial(\Delta\sigma)] (1 + {}_B t_{ij})^{-1/2} \\ &= \left\{ -\frac{\zeta_{ij}}{\eta} + [1 - (\eta \sin\beta + \xi_{ij} \cos\beta)/R] \left(\frac{\sigma}{\eta}\right) \right. \\ &\quad \left. + \frac{1}{2} [1 - S(\eta \sin\beta + \xi_{ij} \cos\beta)/R] \left[ \left(\frac{\omega}{\eta}\right)^2 \left(\frac{\sigma}{\eta}\right) + \left(\frac{\sigma}{\eta}\right)^3 \right] \left(\frac{\eta}{R}\right)^2 \right\} \\ &\quad \times (1 + {}_B t_{ij})^{-1/2} \quad (27) \end{aligned}$$

Second, Equation (29) incorrectly contained a “trailing term” in an attempt to account for the linear gradient in the  $1/\sin\beta$  factor across a curved surface. However, to the extent of consistency with the isolation of different power terms, this effect is already implicit in the formulation of  $\partial B_{ij}/\partial(\Delta\omega)$ . It therefore must not be added post-facto, and the correct equation is simply:

$$i_j x' = \frac{-h\eta}{\sin\beta} \left\{ i_\mu N_{ij} + \left[ \frac{\partial A_{ij}}{\partial(\Delta\omega)} + \frac{\partial B_{ij}}{\partial(\Delta\omega)} \right]_{\omega^{i-1}\sigma^j \text{ coefficient}} \right\} \quad (29)$$

The following related sentence on page 14 of the manuscript is also to be deleted (shown here in strikethrough format): ~~The trailing term in Equation (29) accounts for the linear variation of  $1/\sin\beta$  with  $\omega$  when the optical surface is not flat ( $1/R \neq 0$ ). Coincidentally, the errant addition of that trailing term had exactly nullified the effect of having incorrectly centered the angular coordinates in determining the raytrace extraction points plotted in Figure A1. The correct procedure (rigorously followed in all other raytracings of this manuscript) is to center the linear coordinates. A replacement Appendix A (below) includes the corresponding correction of Equation (A5) and Figure A1. The final results shown in Figure A1 further strengthen the original finding that use of the paraxial image~~

reference in the standard formulation of the light-path expansion is flawed.

The above corrections to the non-paraxial expansion method (introduced by this author) have no effect upon the results for a plane grating. Therefore, the detailed performance values given for the single-element plane grating monochromator were (and remain) exact. However, the present corrections maintain rigor of the author’s general expansion method when applied to curved grating (and mirror) surfaces in the future.

Third, in Equations (69) and (74), the terms  $\tilde{\omega}$  and  $\tilde{\sigma}$  should be replaced by  $(2\tilde{\omega})$  and  $(2\tilde{\sigma})$ , respectively.

## Appendix A (replacement). A Simple Illustration

Figure A1 compares the two light-path calculations (“standard” and “rigorous”) of spherical aberration (4,0) vs. magnification for the simplest and most common focusing optic, namely a spherically concave mirror. The first-degree lateral aberration (“defocus”) vanishes for a mirror radius  $R = 2/[(1 + 1/\eta)\sin\gamma]$ , where  $\gamma$  is the graze angle. Given this constraint, there is no aberration to include in the reference image for calculating the next higher aberration (second-degree “coma”), so the latter result is the same as given by the standard formulation:

$$-{}_{30}x' \frac{\sin\gamma}{\eta} = -\frac{3}{4} \left(1 - \frac{1}{\eta^2}\right) \cos\gamma \sin^2\gamma \quad (A1)$$

Given the same in-focus constraint, the expansion term for spherical aberration simplifies to:

$$-{}_{40}x' \frac{\sin\gamma}{\eta} = e_1 \sin^4\gamma + e_2 \cos^2\gamma \sin^2\gamma \quad (A2)$$

$$\text{where} \quad e_1 = -\frac{1}{8} \left(1 - \frac{1}{\eta} - \frac{1}{\eta^2} + \frac{1}{\eta^3}\right) \quad (A3)$$

$$\text{and} \quad e_2 = \frac{1}{8} \left(9 - \frac{5}{\eta} - \frac{5}{\eta^2} + \frac{9}{\eta^3}\right) \quad (A4)$$

as given by the standard formulation, which employs only the paraxial image reference.

However, to formulate  ${}_{40}x'$  rigorously, one must use Equations (19), (22), (24), (26) and (29) with  $x_{ij} = z_{ij} = 0$  (on-axis point source),  $\alpha = \beta = \gamma$  (mirror),  $\sigma = 0$  (no sagittal rays),  $S = 1$  (spherical surface) and the inclusion therein of the existing lateral ray aberration from Equation (A1) as a non-paraxial image reference point ( $\xi_{40} = {}_{30}x' \omega^2$ ). The resulting equation for  $e_1$  is unchanged compared to the standard result,

due to only the first term of Equation (A2) surviving when  $\gamma = \pi/2$  (normal incidence), and in this case there is no  ${}_{30}x'$  aberration and thus only the standard paraxial image point. However, the rigorous formulation changes the equation for  $e_2$ :

$$e_2 = \frac{1}{8} \left( 6 + \frac{4}{\eta} - \frac{2}{\eta^2} \right) \quad (\text{A5})$$

which yields the same result as Equation (A4) of the standard expansion only for  $\eta = 1$  (where  ${}_{30}x'$  vanishes for all  $\gamma$ ) or  $\eta = 3$  (where  ${}_{30}x' \neq 0$ , but cancels as used in Equation (26)). At all other values of  $\eta$ , the discrepancy is clear from Figure A1 (solid vs. dashed curves). The rigorous theory (and thus the flaw in the standard theory) is confirmed by numerical raytrace extractions, shown as the overlaid data points (solid dots). Due to the high angular aperture (20 mrad), the “uncontaminated” (21-ray) version of Equation (85), employing 7 rays across the pupil meridian at each magnification, was used to insure an accurate extraction of  ${}_{40}x'$ . This agrees precisely with the solid curve resulting from Equations (A2), (A3) and (A5), differing by only negligible amounts (at most,  $1.4 \times 10^{-7}$  mm at a magnification of 0.25).

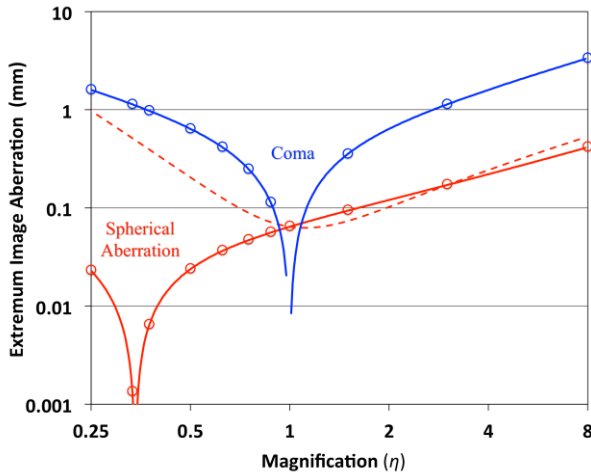


**Fig. A1.** Calculated aberrations of a spherical concave mirror at the Gaussian focus. As the defocus (first-degree) aberration has been forced to vanish by choice of curvature radius, the second-degree (“coma”) aberration is correctly calculated by either the standard or the rigorous light-path formulations. This is confirmed by numerical raytrace results (open circles). However, due to the coma being non-zero at all but unit magnification, the third-degree (“spherical aberration”) lateral ray extremas are shown to be calculated incorrectly by the standard light-path expansion method (dashed curve). The rigorous theory (solid curve), as given in the present work, is seen to agree precisely with independent extractions of this aberration term from numerical raytracings (dots). In this example, the object distance is 1000 mm, the graze angle is  $10^\circ$  and the acceptance aperture is 20 mrad.

From Figure A1, the standard expansion is seen to significantly overcalculate spherical aberration for magnifications  $< 1$ . At grazing angles, this aberration indeed vanishes near the root ( $\eta = 1/3$ ) of the quadratic equation obtained by setting  $e_2 = 0$  in Equation (A5). The standard

formulation incorrectly identifies  ${}_{40}x'$  (“spherical aberration”) as being comparable to  ${}_{30}x'$  (“coma”) at low magnifications. This would result in the combined (e.g. measured) extremum aberration being overestimated by  $\sim 60\%$  at a magnification of 0.25.

Compared to the classic horizontal focusing mirror example given above, the errors inherent in the standard light-path expansion are more significant (at a given numerical aperture) for a surface-normal rotated (off-plane) diffraction grating, and increase further in the presence of varied line-spacing. Firstly, such a geometry gives rise to numerous mixed terms, especially large being those of  $(i,1)$ , and thus a proliferating 2D power matrix of non-paraxial image points. Secondly, the image tilt  $(1,1)$  terms cause a transfer of (otherwise insignificant) vertical aberrations into rotated slit-normal (spectral) components. Thirdly, the inclusion of vertical aberrations as image reference coordinates in the rigorous formulation of the horizontal light-path terms (and vice versa) requires that even non-dominant aberrations be initially calculated accurately to avoid significant errors in the subsequently expanded higher-degree terms. For the above reasons, the standard formulation does not provide an accurate prediction of the aberrations for the new design, or for other off-plane diffraction mountings in non-stigmatic geometries. As specific examples, refer to the discussion in Section 4 and the Table 2 entries for the horizontal aberrations  $x'_{20}$  and  $x'_{21}$ , which are dominant terms of the new optical design and thus require accurate formulation.

## Reference

1. M.C. Hettrick, “A Single-Element Plane Grating Monochromator,” *Photonics* **3**(1), no. 3, 1-44 (2016).